Frog nest foam as a drug delivery system

Sarah Brozio[1], Erin M. O'Shaughnessy[2], Stuart Woods[1], Ivan Hall-Barrientos[1], Patricia E. Martin[2], Malcolm W. Kennedy[3], Dimitrios A. Lamprou[4*] and Paul A. Hoskisson[1*]

[1] Strathclyde Institute of Pharmacy and Biomedical Sciences, University of Strathclyde, 161 Cathedral Street, Glasgow, G4 0RE, UK.

[2] Department of Biological and Biomedical Sciences, School of Health and Life Sciences, Glasgow Caledonian University, G4 OBA, UK.

[3] Institute of Biodiversity Animal Health & Comparative Medicine, Graham Kerr Building, University of Glasgow, Glasgow G12 8QQ, UK.

[4] School of Pharmacy, Queen's University Belfast, 97 Lisburn Road, Belfast BT9 7BL, UK

***Correspondence:** d.lamprou@qub.ac.uk; Paul.hoskisson@strath.ac.uk, Tel.: +44 (0)141 548 2819.

Abstract

Foams have frequently been used as systems for the delivery of cosmetic and therapeutic molecules; however, there is high variability in the foamability and long-term stability of synthetic foams. The development of pharmaceutical foams that exhibit desirable foaming properties, delivering appropriate amounts of the active pharmaceutical ingredient (API) and that have excellent biocompatibility is of great interest. The production of stable foams is rare in the natural world; however, certain species of frogs have adopted foam production as a means of providing a protective environment for their eggs and larvae from a predators and parasites, to prevent desiccation, to control gaseous exchange, temperature extremes, and to reduce UV damage. These foams show great stability (up to 10 days in tropical environments) and are highly biocompatible due to the sensitive nature of amphibian skin. This work demonstrates for the first time, that nests of the Túngara frog (*Engystomops pustulosus*) is stable *ex situ* with useful physiochemical and biocompatible properties and is capable of encapsulating a range of compounds, including antibiotics. These protein foam mixtures may find utility as a topical drug delivery system (DDS).

Keywords: foam; frog; drug delivery; drug release; antibiotics

Introduction

Foams have been used as delivery systems or vehicles to deliver cosmetic and therapeutic molecules to normal and injured skin since the 1970's[1–5]. Yet the long-term stability of liquid aqueous foams has been a challenge, with some formulations offering useful foamability properties (e.g. foam expansion time), but poor stability[6]. There has been some progress made through the combination of various foam and surfactant components to create high foamability and long-term foam stability[6–9]. However, the development of biocompatible, liquid foams with high foamability and long-term stability remains a challenge in materials science[6]. A range of foams is already in use for topical treatments, such as Ibuprofen foams (Biatain® Ib) used to relieve a wide range of exuding wounds, urea-containing foams (KerraFoam) to help alleviate the symptoms of psoriasis, and antibiotic foams containing clindamycin and other antimicrobials such as silver sulfacetamide[2,4]. A major advantage of medicated foams is their ability to cover large surface areas, while containing highly concentrated drugs for topical treatment[1]. One major difficulty can be the delivery of an adequate concentration of active pharmaceutical ingredients (APIs) for treatment over a sustained period, therefore often necessitating repeated, regular applications. In the case of open wounds and burns, regular removal of dressings may lead to increased infection risk and damage to healing surfaces, aid the emergence of antimicrobial resistance through the delivery of sub-minimum inhibitory concentrations of antibiotics, ultimately resulting in reduced infection control and wound healing[10]. Liposomes have proposed for dermatological applications; however, are exhibit major stability issues. There is therefore a need for the development of biomaterials that allow extended times between application combined with high stability and improved biocompatibility; natural foams can provide these benefits.

Anurans (frogs) exhibit enormous diversity in reproductive strategies and styles[11], and many species of tropical and subtropical frog lay their eggs in stable proteinaceous foams that differ in composition between species. Foam-nesting behaviour, thought to have evolved as a means to avoid aquatic predators, prevent desiccation of eggs, control gaseous exchange, buffer temperature extremes, reduce solar radiation damage, and protect eggs from microbial colonisation[12]. Stable biological foams and foam-producing surfactants are rare in nature, presumably due to the requirement for high-energy input for their generation, and the potential of surface-active components to negatively affect cell and membrane function[13,14]. Frog nest foams are remarkable for their strong surfactant activity combined with harmlessness to naked eggs and sperm. The leptodactylid frogs of the neotropics are one such anuran lineage that has

evolved stable foams as an offspring protection mechanism. The nests of the Túngara frog (*Engystomops pustulosus*) are remarkable in structures that act as incubation chambers for eggs[15] (**Supp. Fig. 1A & B;** https://doi.org/10.6084/m9.figshare.13281416.v1), allowing rapid growth and development of embryos, offering a protective environment against predation, whilst providing temperature regulation and oxygen transfer for optimal growth conditions. These nests, there are not destroyed by microbes during larval development despite construction within highly-microbe-rich water[16]. The foam nest structure is highly stable, remaining assembled for as much as 10 days in the tropical environment[17,18], yet the surfactant activity of the foam does not cause damage to the sperm, eggs or developing embryos[13]. The main surfactant protein within these nests is an 11kDa protein, Ranaspumin-2 (RSN-2), which does not disrupt biological membranes or cells, but it still provides sufficient surfactant activity at the air-water interface to allow foam formation[19]. The RSN-2 protein appears to form a clamshell-like structure, which can undergo an unfolding conformational change to expose nonpolar patches on the protein surface to the air, while highly polar regions remain in contact with the water interface to provide the surfactant activity. RSN-2 has been successfully used in industry as a surfactant in nanoparticle production[20], but the use of the whole nest foam protein composition in drug delivery or for tissue engineering applications has not been explored.

Here we show that the unseparated, total protein mixture of *E. pustulosus* nest foam is stable *ex situ* for extended periods with useful physiochemical and biocompatible properties and does not the need of the addition of oxygen as with other drug delivery systems ([21]; DDS) and may be used to encapsulate a range of hydrophobic and hydrophilic model compounds. These data suggest that anuran-derived protein foams may have potential applications as DDSs.

Results & Discussion

Biophysical properties of Tungara frog foam preparation

The composition and properties of DDSs can determine the effectiveness of drug release, and while several factors may affect drug release, the thermodynamics driving the passive diffusion process is key[22]. Thus, increasing and stabilising the local concentration of the permeant is the simplest strategy to facilitate bioavailability[3]. The protein composition of *E. pustulosus* foam fluid was analysed by SDS-PAGE (**Supp. Fig. 1C;** https://doi.org/10.6084/m9.figshare.13281416.v1), confirming previous work that foam from this species contains six major proteins ranging between 10 and 40kDa in size[18] and that the foam nests used in this study were of typical composition. CD spectra of the samples showed a negative maximum at 215 nm and a positive maximum at 194 nm, (**Fig. 1A**) indicating that, cumulatively, the protein mixture in the foam fluid comprises predominately β-sheet structures. Further insight into secondary structure of the foam mixture was obtained by FTIR, which also exhibited spectra consistent with overall dominance of β-sheet structures (**Fig 1B**;[23]). For both foam solutions, transitions were observed at ~1680 cm^{-1}, which are frequencies characteristic of Amide I band, signifying C=O bond stretches typically engaged in β-sheet bonded network structures. These data support previous observations that average secondary structure content of the proteins is predominantly β-sheet[18] and indicates that the centrifugation steps in the preparation of the foam for these experiments does not alter the overall structure and composition of the foam from the wild *E. pustulosus* nests.

Fig. 1

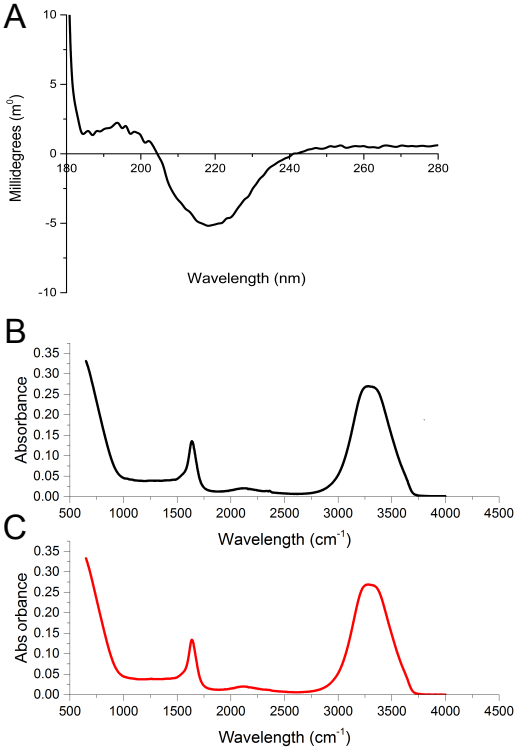

Figure. 1. Structural characterisation of *E. pustulosus* nest foam proteins. 1A: Circular Dichroism of foam fluid using 0.1mm pathlength cuvettes containing 1mg/ml protein foam fluid solution. **1B:** Fourier Transform Infrared Spectroscopy (FTIR) foam fluid **(B)** and whole foam **(C)**. For both CD and FTIR spectra were corrected for baseline and buffer effects each measurement was carried out in triplicate and the mean of the data is presented.

To investigate the viscoelastic properties of the foam, oscillation sweep experiments were employed by rheology. The whole foam fluid was found to tolerate up to 100 Pa of shear stress force before it reaches a breaking point, at which the elastic modulus of the foam decreases and foam structure and stability is lost (**Fig. 2A**). Time sweep experiments indicated that up to 1500 s the foam preparation moduli are unchanged by stress and frequency. After 1500 s both elastic and viscosity moduli increase demonstrating that water is being lost from the foam (**Fig. 2B**). It has been suggested that stress increases the chances of water loss from the foam followed by coarsening, which leads to an increase in viscoelasticity[24]. The *E. pustulosus* whole foam is able to withstand shear stress and pressure before breaking down, demonstrating the long-lasting stability that may be observed in nature. Pharmaceutical foams are typically required to remain stable in order to be properly manipulated while being applied, but have low shear allowing them to break down shortly thereafter[25,26]. The foam derived from *E. pustulosus*

has exhibits long-term stability in harsh tropical environments (e.g. heat, high level exposure to ultraviolet light, and physical disruption) and behaves differently from typical pharmaceutical foams[2]. The *E. pustulosus* foam is stable enough to be manipulated and able to withstand shear forces, giving the potential to deliver drugs over prolonged periods.

Fig. 2

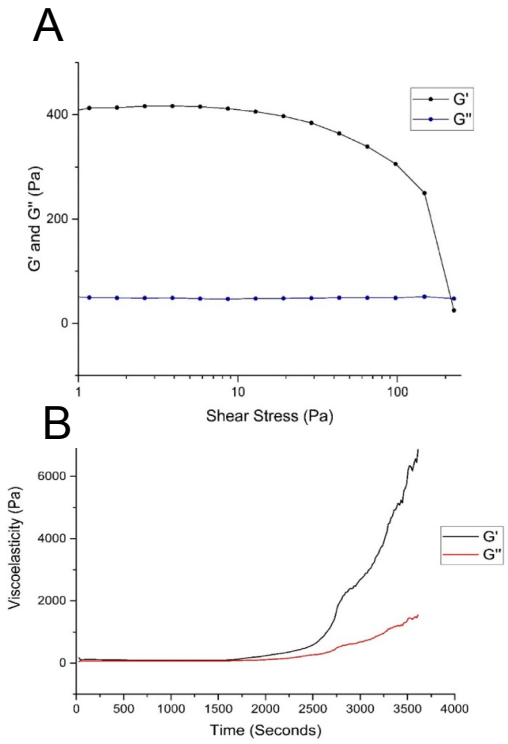

Figure 2. Viscoelastic properties of *E. pustulosus* nest foam. 2A: Time sweep rheology data for foam, showing both elastic (G') and viscous (G'') moduli. Stress was set at 100 Pa, and carried out over 1 hour. **2B:** Oscillation sweep rheology data for *E. pustulosus* foam, showing both elastic (G') and viscous (G'') moduli. Shear stress was increased from 1 Pa to 200 Pa. Each measurement was taken in triplicate at 20^0C.

Frog foam biocompatibility with human epithelial cells

To investigate the susceptibility of mammalian cells to any possible toxic effects of the foam, cells were cultured in the presence of foam fluid and potential toxicity was assayed using an MTT-based cell viability assay. Exposing HaCaT keratinocyte cells to a range of *E. pustulosus* foam concentrations did not affect the overall cell viability and multiplication of the cells (**Fig. 3**). The higher foam fluid concentrations to which the cells were exposed are representative of foam concentration present in *E. pustulosus* nests (1-2mg/ml protein[17]). Cells exposed to the foam behave in the same manner as untreated control cells, demonstrating that the foam proteins from *E. pustulosus* are non-toxic to epithelial cells and are therefore unlikely to cause damage to the skin or underlaying tissues if used as a topical drug delivery system. The foam and its protein components are already known to be harmless to human erythrocytes [27]. This high degree of biocompatibility is consistent with the foam and its precursor components being harmless to naked amphibian sperm, eggs, and oviduct surfaces of the frogs[27].

Fig. 3

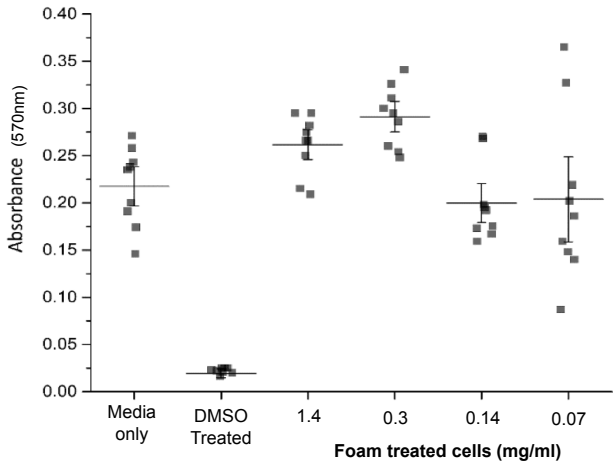

Fig. 3. Biocompatibility of *E. pustulosus* nest foam with human epithelial cells. MTT assay of HaCaT cell viability following exposure to a range of fluid foam concentrations over 24 hours at 37^0C. Each treatment was performed in triplicate, and media alone was used as normal viability control, and cells were treated with DMSO for non-viable control. Treatments 1 to 4 were a dilution of fluid foam protein concentrations - 1.4 mg/ml, 0.3 mg/ml, 0.14 mg/ml and 0.07 mg/ml respectively. Error bars represent the standard deviation of the data about the mean (horizontal line).

In vitro release of drug-loaded frog foam

A single foam cell is defined as a bubble of gas enclosed in a liquid film that can be polyhedral or circular, heterogeneous or homogeneous, and usually range between 0.1 and 3mm in diameter[25]. The cell structure of *E. pustulosus* nest-foam was evaluated microscopically and the foam cell sizes measured (**Fig. 4A**). The foam cells in all samples were found to be a heterogeneous mixture of uneven, spherical and polyhedral cells with a Feret diameter ranging from 10-800 μm, falling in the normal range of foam cell size of foams that have been used previously in pharmaceutical applications[25].

The relative density of the foam was found to be 0.25 g of protein/ml. AFM PeakForce analysis of the fluid foam and gel foam indicated consistency of the individual adhesion force (F_{ad}) measurements in each foam forms (**Fig. 4B**) indicating that the foam surface forces are homogeneous across the surface of each form. Moreover, in the case of the fluid foam, the F_{ad} is higher and the AFM images shows the formation of ~200 nm droplets as the foam was dried on to mica surfaces. This combination of low density and high structural stability is unusual and could suggest the utility of anuran foam-nest proteins as a pharmaceutical foam.

Fig. 4

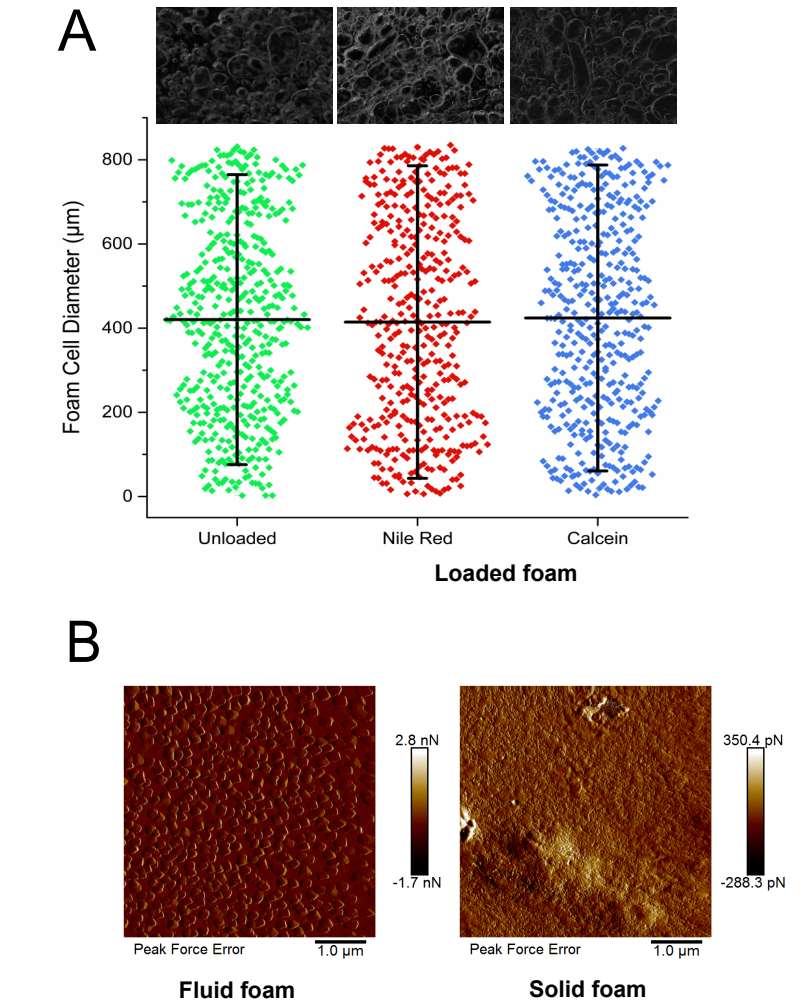

Fig. 4. Drug loading of *E. pustulosus* nest foam does not alter the structure of the foam. **4A**. Foam cell diameter measurements scatter plot. Feret diameter of each foam cell/bubble was measured using Fiji software. Bars on the scatter encompass 10-90% of the data points, with the central horizontal line representing mean values. Above the scatter graph are representative images of unloaded foam, foam loaded with 1 mg/ml NR and foam loaded with 1mg/ml calcein. All images were taken using freshly defrosted foam. **4B.** Atomic Force Microscopy PeakForce analysis of foam fluid and gel foam to investigate the consistency of the adhesion force (F_{ad}) in the foam.

To evaluate the drug release behaviour of *E. pustulosus* foam, experiments were performed using a dialysis-based method where two model compounds (one hydrophobic and one hydrophilic), NR and calcein, were encapsulated in the foams. Calcein exhibits a "burst-type" release profile from the foam, whereas NR is discharged at a linear rate over 168 hours (**Fig. 5A & B**). These data indicate that the whole foam can absorb and release both hydrophobic (NR) and hydrophilic (calcein) molecules and release these at different rates over a prolonged period, with up to 85% of the loaded dye released over a period of 168 hours. Moreover, the loading of the nest foam with NR or calcein did not alter the cell size or shape of the foam (**Fig.** 4).

To test the ability of the foam to release a clinically relevant drug molecule, the whole foam loaded in the same manner as for the previous two molecules with the red-pigmented antibiotic rifampicin. The dialysis method of release showed that rifampicin was released at a steady rate over the first five hours with a release of around 80% of loaded antibiotic, followed by a second, slower phase of release (**Fig. 5C**).

To further investigate the release of drug molecules from *E. pustulosus* foam, a novel trans-well-based release assay was developed, which emulates delivery of the foam preparation across a more complex protein coated surface. Foam was loaded in to a collagen-coated transwell sat in a 24-well tissue culture plate containing 1 ml of PBS and release of drug molecule was determined through the assay of the amount of rifampicin that passed from the foam through the transwell membrane. In the transwell assay, around 50% of rifampicin was also released over a 48 hrs (**Fig. 5D**). This novel transwell assay for investigating compound release from foams offers a simpler route to assaying drug release from foams and other aqueous-based materials that does not require the manipulation of dialysis tubing. Moreover, the release mimics clinical applications through release from a single face of the transwell (A schematic of the Transwell-based assay is provided in **Fig. 5E**) with the advantage that transwells are available in a number of sizes and pore diameters to suit a range of needs.

These data indicate that the foam can be loaded with drug molecules and can be used as an extended release system. The foam from *E. pustulosus* is stable and the API release is relatively slow with the foam potentially acting as a barrier in the local environment. The *E. pustulosus* foam compares well with release of rifampicin from loaded nanoparticles where 80-90% of release occurs, but within an 8 h time window[28].

Fig. 5

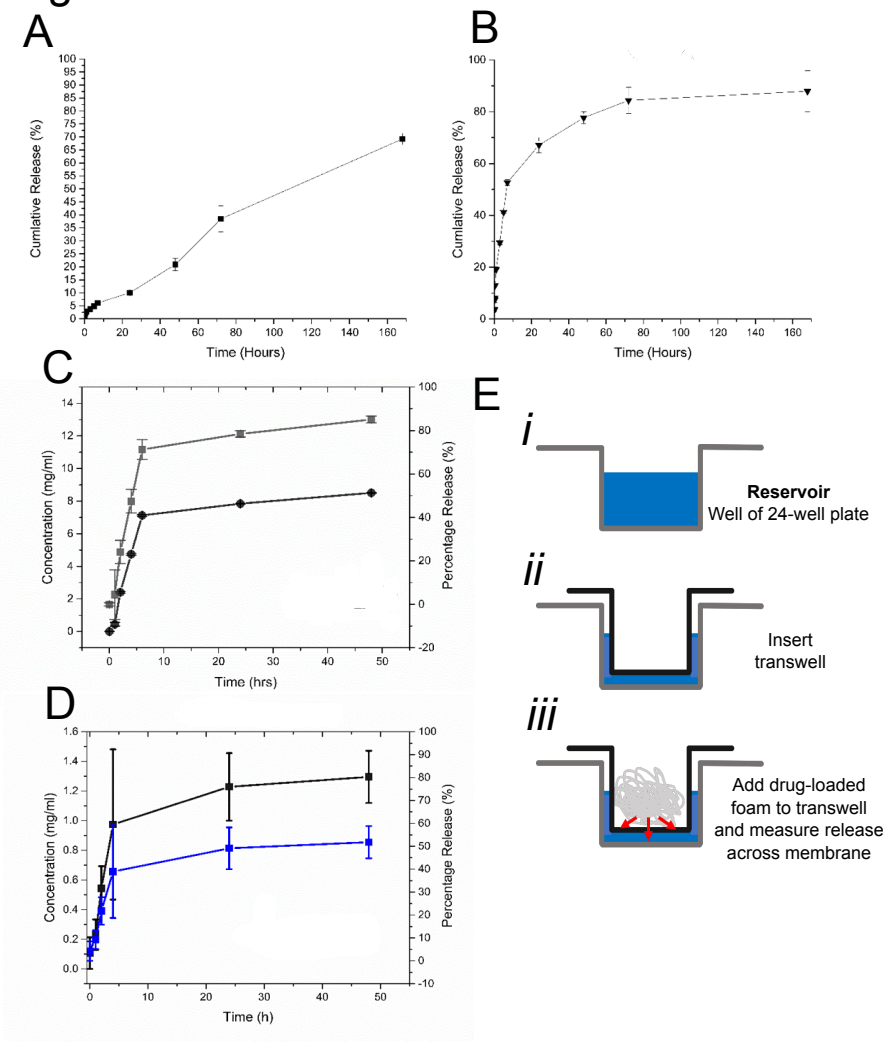

Fig. 5. *E. pustulosus* nest foam can take up and release model compounds and drug molecules. 5A: Cumulative release of the dye NR from loaded whole foam over 168 hrs using the dialysis method. **5B:** Cumulative release of the dye calcien from loaded whole foam over 168 hrs using the dialysis method. **5C:** Cumulative release of the antibiotic rifampicin from loaded whole foam over 168 hrs using the dialysis method; -●- concentration (mg/ml); -■- percentage release of the dye or drug. **5D:** Release of rifampicin using novel transwell method; -■- concentration (mg/ml of protein); -■- percentage release of rifampicin. Each point represents the mean of data collected in triplicate and error bars indicate the standard deviation of the data. Sink conditions satisfied by replacing sample volume with fresh buffer at each sample point. Dye release concentrations were calculated using spectrophotometric standard curves for respective dye or drug. **5E:** Schematic representing the experimental set-up using the novel transwell release assay, with reservoirs of 24-well plate filled with buffer **(*i*)**, the insertion of the permeable transwell **(*ii*)**, and the addition of drug-loaded foam to the transwell to allow drug release across the transwell membrane which can be quantified in the reservoir.

Many nanoparticle-based systems release their drug-load rapidly resulting in ineffective long-term treatment possibilities[29] and have shown to exhibit some toxic properties[30]. The anuran foam-based preparations extend this release period to around 48 hrs depending on the nature of the compounds used, expanding the possible utility of these foam systems. While there has been multiple antibiotic loaded liposomes[31–33](AmBisome, Lambin, Doxil) brought to market, little have transferred the applicability to topical conditions, and their efficiency is still lacking. Further, tetracycline loaded nanocomposite hydrogels have been presented as for extended release delivery through the skin, released of maximum of 15% of the loaded antibiotic[32]. Foams are considered more popular with patients than gels[2], and a stable foam may provide a solution to both these issues. Previous studies of pharmaceutical foams have investigated the immediate delivery of drugs through to the dermis by exploiting the fast breakdown of foam preparations, but rarely have they been used for long-term drug release[2]. The foam derived from *E. pustulosus* provides a material with intermediate release properties, where uptake is efficient, its high stability and slow release properties enable continuous release over a clinically useful period of time.

Conclusions

There is an increased interest in drug delivery systems to refine the use of antimicrobial drugs currently available on the market, which may enable novel delivery systems help combat the rise of antimicrobial resistance in the clinic. Anuran foams from reproductive nests may provide a novel area for investigation in the area of controlled release. Anuran foam nests are highly biocompatible, durable and stable, and have excellent drug release properties. They exhibit none of the issues associated with fabric-based drug release such as instability, rapid release characteristics or toxicity. These advantages suggest that anuran foam may provide a novel topical drug delivery system for controlled release of drugs.

Materials and Methods

Materials

Nile red (NR), calcein, ethanol 97% (v/v), phosphate buffered saline (PBS) tablets (pH 7.2) were all purchased from Sigma and MTT (3-(4,5-dimethylthiazol-2-yl)-2,5-diphenyltetrazolium was purchased from Thermofisher.

Collection of *Engystomops pustulosus* foam

Freshly laid foam nests or adult frogs in amplexus (allowed to lay in captivity, before release) were collected from a number of sites in northern Trinidad in June and July of 2014, 2015 and 2016. Nests were removed from the surface of the water in which they were produced and the eggs were removed manually before being stored at -20^{0}C for transfer to the Glasgow, where they were stored at -80^{0}C. Foam was freshly defrosted for all experiments. Soluble foam material ('foam fluid') was produced by centrifuging whole foam for 10 min (16,000 x *g*), providing a solution with approximately ~2 mg/ml protein. This also yields a supernatant/pellicle residual of semi-solid compressed foam ('gel foam') on top of the foam fluid layer.

Microscopy

Optical microscopy: Whole foam was defrosted at room temperature before use. All foam images were taken using transmitted light on a Nikon SMZ1500 stereomicroscope with images acquired using a DFK 33UX264 CMOS camera (The Imaging Source Europe GmbH, Germany) using NIS-Elements AR.3.2 software. Fiji software (https://fiji.sc/) from the ImageJ (https://imagej.net) package was used for image analysis.

Atomic force microscopy (AFM): Samples (5 µl) of foam were deposited onto a freshly cleaved mica surface (1.5 cm x 1.5 cm; G250-2 Mica sheets 25 mm x 25 mm x 0.15 mm; Agar Scientific Ltd, Essex, UK) and left to dry at room temperature for 1h before imaging. The images were obtained by scanning the mica surface in air under ambient conditions using a Scanning Probe Microscope (MultiMode® 8, Digital Instruments, Santa Barbara, CA, USA; Bruker Nanoscope analysis software Version 1.40), operating using the PeakForce QNM mode. The AFM measurements were obtained using ScanAsyst-air probes, for which the spring constant (0.58 N/m; Nominal 0.4 N/m) and deflection sensitivity had been calibrated, but not the tip radius (the nominal value used was 2 nm).

Sodium Dodecyl Sulfate Poly-Acrylamide Gel Electrophoresis (SDS-PAGE)

Solid and liquid foam samples were electrophoresed on precast NuPAGE 15% polyacrylamide Bis-Tris gels (Invitrogen) at 120V using 4 X SDS reducing loading buffer (Invitrogen). Each gel was stained with InstaBlue Coomassie protein stain for ~45 min.

Circular Dichroism Spectroscopy (CD)

CD was used to investigate the overall secondary structure content of the proteins. Spectra were acquired using a Chirascan Plus (Applied Photophysics) instrument using a 0.1mm quartz cuvette (Hellma) at 20^0C. All samples (10 mg/ml protein) were measured in the far-UV in a wavelength range of 180 nm to 280 nm range, with step size of 1 nm, bandwidth of 1 nm, and reading time of 1 s per nm. Triplicate measurements were taken for each sample run, baseline peak, PBS control and foam sample spectra, with triplicate spectra then averaged. Baseline and PBS traces where subtracted from the sample spectra before secondary structure predictions were made. All data analysis was performed using Global3 software and Excel.

Fourier transform infrared spectroscopy

Fourier transform infrared (FTIR) spectroscopy was carried out using a Nicolet iS10 Smart iTR spectrophotometer (Thermo Scientific). Solid and liquid foam spectra were recorded in the range on 4000 cm^{-1} and 500 cm^{-1}, over 128 scans at a resolution of 4 cm^{-1} and an interval of 1 cm^{-1}. Background spectra were measured and the foam spectra were corrected accordingly.

Rheology

Rheology measurements were determined using a HAAKE MARS Rotational Rheometer (Thermo Scientific). Foam samples were subjected to oscillation sweeps and time sweeps. All experiments were carried out using P20 upper plate and TM20 lower plate. The oscillation sweeps were completed with a 1 mm gap and 0.1 Pa to 200 Pa range. Time sweep experiments were run for 1 h, at 100 Pa and 3 Hz using a 0.5 mm gap. Data points were collected in triplicate and averaged before analysis was carried out.

MTT cell viability assay

HaCaT cells (CLS, Eppelheim, Germany), a model human keratinocyte cell line were cultured in Dulbecco's modified Eagle's medium (DMEM) containing 4.5 g/l glucose supplemented with 10% (v/v) fetal bovine serum, 2 mM L-glutamine and 50 units/ml penicillin/streptomycin (cDMEM; Lonza, Slough, UK). Soluble foam proteins were prepared as above, with the supernatant being passed the a 0.22 μm filter (Millex 33 mm) and subsequently concentrated

using an Amicon 10 kDa spin filter. The protein concentration was determined by Bradford assay (BioRad). The HaCaT cells were plated onto 96 well plates (~1x10^3 cells per well and grown to 80% confluence) and were treated with buffer containing foam proteins (concentrations indicated in the figures) prior to incubation at 37 ^{0}C for 24 hours. After 24 hours the media was removed from the cells, and replaced with 50 µl of fresh media and 50 µl of MTT (5mg/ml) and incubated for 1 h at 37 ^{0}C. This was followed by replacing the media with 100 µl DMSO and further incubation in the dark at room temperature for 30 minutes prior to reading the absorbance at 570nm[34]. Results were expressed as the % viability compared to non-treated cells ± SEM.

In vitro release of model compounds

Aliquots (500 mg) of whole foam were loaded with dye by mixing with either 400 µl of Nile Red (NR; hydrophobic; 1 mg/ml in ethanol) or calcein (hydrophilic; 1 mg/ml in ethanol). The mixture was the placed in dialysis tubing and sealed before being submerged in 10 ml PBS at 37 ^{0}C (pH 7; for NR-based release experiments, a 1:1 mixture of ethanol and PBS was used). The release experiments were carried out at 37 ^{0}C, over 168 hours. To satisfy the perfect-sink conditions, which allow for the determination of the diffusion parameters, the supernatant was replaced with fresh PBS at 37 °C at each time point (indicated in the graphs). The concentration of model compound in each sample was determined spectrophotometrically at 490 nm (calcein) or 590 nm (NR) and the concentration determined with reference to standard control calibration curves. Experiments were performed in triplicate.

In vitro Antibiotic release

Two *in vitro* techniques were used to investigate the release of the antibiotic rifampicin.

Dialysis: Aliquots (400 mg) of foam were mixed with 400 µl of rifampicin (25 mg/ml). The loaded foam was placed into dialysis tubing, sealed and submerged in 10 ml of PBS. This was incubated at 37 ^{0}C for 48 hours. Samples (1 ml) were taken and fresh media added to maintain sink conditions. Samples where measured by spectrophotometrically at 475 nm[35] against a calibration curve.

Transwell: Aliquots of foam (100 mg) were loaded with 100 µl of rifampicin (25mg/ml). Loaded foam was the placed into a transwell collagen-coated permeable support (0.4 µm; Nunc). Each support was inserted into 24 well plate well containing 600ul of PBS. The plate

was then incubated for 48 hours at 37 ^{0}C. PBS (600µl) was collected from a well for each time point, and the absorbance measured at 475nm, in triplicate.

383 **Supporting Information**.

384 **Supplementary Figure** https://doi.org/10.6084/m9.figshare.13281416.v1; **Fig. 1A.** Adult
385 Túngara frog (*Engystomops pustulosus*). **B.** *In situ E. pustulosus* foam nest. **C.** SDS-PAGE gel
386 of *E. pustulosus* whole foam from a wild-collected nest electrophoresed

387 **Acknowledgements**

388 The authors would like to acknowledge the Engineering and Physical Science Research Council
389 (EPSRC) via the Doctoral Training Centre (DTC) at the University of Strathclyde for the PhD
390 studentship support to SB. We would also like to thank Prof. Roger Downie, University of
391 Glasgow for his long-term assistance in the field and advice on Tungara Frogs. We
392 acknowledge the support of the Microbiology Society and the Pauline Fitzpatrick Memorial
393 Travel Fund to SB to support fieldwork in Trinidad. EMO was supported by a PhD studentship
394 from the Psoriasis Association (ST3 15).
395 We would also like to thank the Wildlife Section, Forestry Division, of the Government of
396 Trinidad and Tobago for issuing Special Game Licences under the Conservation of Wildlife
397 Act, permitting us to collect *E. pustulosus* nests (Special Game Licences 2014-2016 and
398 Wildlife Special Export Licence numbers: 001741, 001161 and 000646).
399

400 **Conflict of interest**

401 All authors declare that they have no conflict of interest in relation to this work.

References

1. Haznar-Garbacz D, Garbacz G, Weitschies W. 2019 Development of oral foams for topical treatment of inflammatory bowel disease. *J Drug Deliv Sci Tec* **50**, 287–292. (doi:10.1016/j.jddst.2019.01.022)

2. Zhao Y, Jones SA, Brown MB. 2010 Dynamic foams in topical drug delivery. *J Pharm Pharmacol* **62**, 678–84. (doi:10.1211/jpp.62.06.0003)

3. Gennari CGM, Selmin F, Minghetti P, Cilurzo F. 2019 Medicated foams and film forming dosage forms as tools to improve the thermodynamic activity of drugs to be administered through the skin. *Curr Drug Deliv* **16**, 461–471. (doi:10.2174/1567201816666190118124439)

4. Zhao Y, Brown MB, Jones SA. 2010 Pharmaceutical foams: are they the answer to the dilemma of topical nanoparticles? *Nanomed Nanotechnol Biology Medicine* **6**, 227–236. (doi:10.1016/j.nano.2009.08.002)

5. Svagan AJ, Benjamins J-W, Al-Ansari Z, Shalom DB, Müllertz A, Wågberg L, Löbmann K. 2016 Solid cellulose nanofiber based foams - Towards facile design of sustained drug delivery systems. *J Control Release Official J Control Release Soc* **244**, 74–82. (doi:10.1016/j.jconrel.2016.11.009)

6. Russo M, Amara Z, Fenneteau J, Chaumont-Olive P, Maimouni I, Tabeling P, Cossy J. 2020 Stable liquid foams from a new polyfluorinated surfactant. *Chem Commun* (doi:10.1039/d0cc02182b)

7. Fameau A-L *et al.* 2011 Smart Foams: Switching Reversibly between Ultrastable and Unstable Foams. *Angewandte Chemie Int Ed* **50**, 8264–8269. (doi:10.1002/anie.201102115)

8. Arriaga LR, Drenckhan W, Salonen A, Rodrigues JA, Íñiguez-Palomares R, Rio E, Langevin D. 2012 On the long-term stability of foams stabilised by mixtures of nano-particles and oppositely charged short chain surfactants. *Soft Matter* **8**, 11085. (doi:10.1039/c2sm26461g)

9. Stocco A, Carriere D, Cottat M, Langevin D. 2010 Interfacial Behavior of Catanionic Surfactants. *Langmuir* **26**, 10663–10669. (doi:10.1021/la100954v)

10. Heunis TDJ, Dicks LMT. 2010 Nanofibers offer alternative ways to the treatment of skin infections. *J Biomed Biotechnology* **2010**, 510682. (doi:10.1155/2010/510682)

11. Crump ML. 2015 Anuran Reproductive Modes: Evolving Perspectives. *J Herpetol* **49**, 1–16. (doi:10.1670/14-097)

12. Pereira EB, Pinto-Ledezma JN, Freitas CG de, Villalobos F, Collevatti RG, Maciel NM. 2017 Evolution of the anuran foam nest: trait conservatism and lineage diversification. *Biol J Linn Soc* **122**, 814–823. (doi:10.1093/biolinnean/blx110)

13. Cooper A, Kennedy MW. 2010 Biofoams and natural protein surfactants. *Biophys Chem* **151**, 96–104. (doi:10.1016/j.bpc.2010.06.006)

14. Cooper A, Vance SJ, Smith BO, Kennedy MW. 2017 Frog foams and natural protein surfactants. *Colloids Surfaces Physicochem Eng Aspects* **534**, 120–129. (doi:10.1016/j.colsurfa.2017.01.049)

15. Downie, R J. 1988 Functions of the foam in the foam-nesting leptodactylid Physalaemus pustulosus. *The Herpetological Journal* **1**, 302–307.

16. Downie, R. J. 1990 Functions of the foam in foam-nesting leptodactylids anti-predator effects of Physalaemus pustulosus foam. **1**, 501–503.

17. Fleming RI, Mackenzie CD, Cooper A, Kennedy MW. 2009 Foam nest components of the túngara frog: a cocktail of proteins conferring physical and biological resilience. *Proceedings of the Royal Society B: Biological Sciences* **276**. (doi:10.1098/rspb.2008.1939)

18. Cooper A, Kennedy MW, Fleming RI, Wilson EH, Videler H, Wokosin DL, Su T, Green RJ, Lu JR. 2005 Adsorption of Frog Foam Nest Proteins at the Air-Water Interface. *Biophys J* **88**, 2114–2125. (doi:10.1529/biophysj.104.046268)

19. Mackenzie CD, Smith BO, Meister A, Blume A, Zhao X, Lu JR, Kennedy MW, Cooper A. 2009 Ranaspumin-2: Structure and Function of a Surfactant Protein from the Foam Nests of a Tropical Frog. *Biophysical Journal* **96**. (doi:10.1016/j.bpj.2009.03.044)

20. Choi H-J, Ebersbacher CF, Myung NV, Montemagno CD. 2012 Synthesis of nanoparticles with frog foam nest proteins. *J Nanopart Res* **14**, 1092. (doi:10.1007/s11051-012-1092-1)

21. Suvarnapathaki S, Wu X, Lantigua D, Nguyen MA, Camci-Unal G. 2019 Breathing life into engineered tissues using oxygen-releasing biomaterials. *Npg Asia Mater* **11**, 65. (doi:10.1038/s41427-019-0166-2)

22. Freire MCLC, Jr. FA, Marcelino HR, Picciani PH de S, Silva KG de H e, Genre J, Oliveira AG de, Egito EST do. 2017 Understanding Drug Release Data through Thermodynamic Analysis. *Materials* **10**, 651. (doi:10.3390/ma10060651)

23. KONG J, YU S. 2007 Fourier Transform Infrared Spectroscopic Analysis of Protein Secondary Structures. *Acta Bioch Bioph Sin* **39**, 549–559. (doi:10.1111/j.1745-7270.2007.00320.x)

24. Marze SPL, Saint-Jalmes A, Langevin D. 2005 Protein and surfactant foams: linear rheology and dilatancy effect. *Colloids Surfaces Physicochem Eng Aspects* **263**, 121–128. (doi:10.1016/j.colsurfa.2005.01.014)

25. Arzhavitina A, Steckel H. 2010 Foams for pharmaceutical and cosmetic application. *Int J Pharmaceut* **394**, 1–17. (doi:10.1016/j.ijpharm.2010.04.028)

472 26. Kealy T, Abram A, Hunt B, Buchta R. 2007 The rheological properties of pharmaceutical
473 foam: implications for use. *Int J Pharmaceut* **355**, 67–80.
474 (doi:10.1016/j.ijpharm.2007.11.057)

475 27. Clark BT. 2007 The natural history of Amphibian skin secretions, their normal
476 functioning and potential medical applications. *Biol Rev* **72**, 365–379. (doi:10.1111/j.1469-
477 185x.1997.tb00018.x)

478 28. Sung JC, Padilla DJ, Garcia-Contreras L, Verberkmoes JL, Durbin D, Peloquin CA,
479 Elbert KJ, Hickey AJ, Edwards DA. 2009 Formulation and pharmacokinetics of self-
480 assembled rifampicin nanoparticle systems for pulmonary delivery. *Pharmaceut Res* **26**,
481 1847–55. (doi:10.1007/s11095-009-9894-2)

482 29. Sabaeifard P, Abdi-Ali A, Soudi MR, Gamazo C, Irache JM. 2016 Amikacin loaded
483 PLGA nanoparticles against Pseudomonas aeruginosa. *European J Pharm Sci Official J*
484 *European Fed Pharm Sci* **93**, 392–8. (doi:10.1016/j.ejps.2016.08.049)

485 30. Toppo FA, Pawar RS. 2015 Novel drug delivery strategies and approaches for wound
486 healing. **2**, 12-20.

487 31. Azanza JR, Sádada B, Reis J. 2015 Liposomal formulations of amphotericin B:
488 differences according to the scientific evidence. *Revista Española De Quimioterapia*
489 *Publicación Oficial De La Sociedad Española De Quimioterapia* **28**, 275–81.

490 32. Namazi H, Rakhshaei R, Hamishehkar H, Kafil HS. 2016 Antibiotic loaded
491 carboxymethylcellulose/MCM-41 nanocomposite hydrogel films as potential wound dressing.
492 *Int J Biol Macromol* **85**, 327–334. (doi:10.1016/j.ijbiomac.2015.12.076)

493 33. Lee M-K. 2019 Clinical usefulness of liposomal formulations in cancer therapy: lessons
494 from the experiences of doxorubicin. *J Pharm Investigation* **49**, 203–214.
495 (doi:10.1007/s40005-018-0398-0)

496 34. Niles AL, Moravec RA, Worzella TJ, Evans NJ, Riss TL. 2013 High-Throughput
497 Screening Methods in Toxicity Testing. , 107–127. (doi:10.1002/9781118538203.ch5)

498 35. Benetton SA, Kedor-Hackmann ERM, Santoro MIRM, Borges VM. 1998 Visible
499 spectrophotometric and first-derivative UV spectrophotometric determination of rifampicin
500 and isoniazid in pharmaceutical preparations. *Talanta* **47**, 639–643. (doi:10.1016/s0039-
501 9140(98)00111-8)

502

503

Figure legends

Fig. 1. Structural characterisation of *E, pustulosus* nest foam proteins. 1A: Circular Dichroism of foam fluid using 0.1mm pathlength cuvettes containing 1mg/ml protein foam fluid solution. **1B:** Fourier Transform Infrared Spectroscopy (FTIR) foam fluid **(B)** and whole foam **(C)**. For both CD and FTIR spectra were corrected for baseline and buffer effects each measurement was carried out in triplicate and the mean of the data is presented.

Fig. 2. Viscoelastic properties of *E. pustulosus* nest foam. 2A: Time sweep rheology data for foam, showing both elastic (G') and viscous (G'') moduli. Stress was set at 100 Pa, and carried out over 1 hour. **2B:** Oscillation sweep rheology data for *E. pustulosus* foam, showing both elastic (G') and viscous (G'') moduli. Shear stress was increased from 1 Pa to 200 Pa. Each measurement was taken in triplicate at 20^0C.

Fig. 3. Biocompatibility of *E. pustulosus* nest foam with human epithelial cells. MTT assay of HaCaT cell viability following exposure to a range of fluid foam concentrations over 24 hours at 37^0C. Each treatment was performed in triplicate, and media alone was used as normal viability control, and cells were treated with DMSO for non-viable control. Treatments 1 to 4 were a dilution of fluid foam protein concentrations - 1.4 mg/ml, 0.3 mg/ml, 0.14 mg/ml and 0.07 mg/ml respectively. Error bars represent the standard deviation of the data about the mean (horizontal line).

Fig. 4. Drug loading of *E. pustulosus* nest foam does not alter the structure of the foam. 4A. Foam cell diameter measurements scatter plot. Feret diameter of each foam cell/bubble was measured using Fiji software. Bars on the scatter encompass 10-90% of the data points, with the central horizontal line representing mean values. Above the scatter graph are representative images of unloaded foam, foam loaded with 1 mg/ml NR and foam loaded with 1mg/ml calcein. All images were taken using freshly defrosted foam. **4B.** Atomic Force Microscopy PeakForce analysis of foam fluid and gel foam to investigate the consistency of the adhesion force (F_{ad}) in the foam.

Fig. 5. *E. pustulosus* nest foam can take up and release model compounds and drug molecules. 5A: Cumulative release of the dye NR from loaded whole foam over 168 hrs using the dialysis method. **5B:** Cumulative release of the dye calcien from loaded whole foam over 168 hrs using the dialysis method. **5C:** Cumulative release of the antibiotic rifampicin from loaded whole foam over 168 hrs using the dialysis method; -●- concentration (mg/ml); -■-

percentage release of the dye or drug. **5D:** Release of rifampicin using novel transwell method; -■- concentration (mg/ml of protein); -■- percentage release of rifampicin. Each point represents the mean of data collected in triplicate and error bars indicate the standard deviation of the data. Sink conditions satisfied by replacing sample volume with fresh buffer at each sample point. Dye release concentrations were calculated using spectrophotometric standard curves for respective dye or drug. **5E:** Schematic representing the experimental set-up using the novel transwell release assay, with reservoirs of 24-well plate filled with buffer **(*i*)**, the insertion of the permeable transwell **(*ii*)**, and the addition of drug-loaded foam to the transwell to allow drug release across the transwell membrane which can be quantified in the reservoir.

Supplementary Figure https://doi.org/10.6084/m9.figshare.13281416.v1

Supplementary Fig. 1A. Adult Túngara frog (*Engystomops pustulosus*). **B.** *In situ E. pustulosus* foam nest. **C.** SDS-PAGE gel of *E. pustulosus* whole foam from a wild-collected nest electrophoresed through a 4-20% Tris-Glycine NuPAGE gel under reducing conditions. Proteins in the 10-30 kDa range are the ranaspumins (RSN described by Fleming et al., 2009 - highlighted by red boxes. RSN molecular mass based on amino acid sequence: RSN-1, 14kDa; RSN-2, 11kDa; RSN-3, 18kDa; RSN-4, 21kDa; RSN-5, 18kDa; RSN-6, 27kDa) **Marker:** 10-200kDa Broad Range marker (New England Biolabs; #P7704).

Reference

Fleming, R. I., C.D. Mackenzie, A. Cooper, M.W. Kennedy, Foam nest components of the Túngara frog: a cocktail of proteins conferring physical and biological resilience, Proceedings of the Royal Society B: Biological Sciences. 276 (2009). doi:10.1098/rspb.2008.1939**.**